Temperature-Dependent Structural Properties, Phase Transition Behaviour and Dynamic Properties of a Benzene Derivative in the Solid State

Yating Zhou,[1] Rhian Patterson,[1] P. Andrew Williams,[1] Benson M. Kariuki,[1] Colan E. Hughes,[1] Ranita Samanta,[2] Ramesh Devarapalli,[2] C. Malla Reddy,[2] David C. Apperley,[3] Kenneth D. M. Harris[1]*

1 School of Chemistry, Cardiff University, Park Place, Cardiff CF10 3AT, Wales.

2 Department of Chemical Sciences, Indian Institute of Science Education and Research Kolkata, Mohanpur 741246, West Bengal, India.

3 Department of Chemistry, University of Durham, South Road, Durham DH1 3LE, England.

* Author for correspondence: HarrisKDM@cardiff.ac.uk

Abstract

We report the solid-state structural properties and phase transition behaviour of 1,4-dibromo-2,3,5,6-tetramethylbenzene, demonstrating that this material undergoes an order-disorder phase transition below ambient temperature (at *ca.* 154 K on cooling and *ca.* 160 K on heating). In both the high-temperature and low-temperature phases, the crystal structure is based on π-stacking of the molecules. In the crystal structure of the high-temperature phase, the bromine occupancy in each substituent site is *ca.* 1/3 and the methyl group occupancy in each substituent site is *ca.* 2/3, consistent with statistical orientational disorder of the molecule between six distinct orientations. Natural-abundance solid-state ^{2}H NMR spectroscopy confirms that, at ambient temperature, this disorder is dynamic *via* rapid molecular reorientation about an axis perpendicular to the aromatic ring. In the low-temperature phase, the bromine and methyl substituents occupy preferred sites within the crystal structure, with the distribution of site occupancies becoming progressively more ordered on decreasing temperature.

1. Introduction

The phenomenon of polymorphism, the existence of multiple crystalline forms with identical chemical composition but different crystal structures, is a widely studied topic.[1,2] Under a given set of physical conditions, only one polymorph is thermodynamically stable, and the other polymorphs are meta-stable. On changing the physical conditions (for example, by variation of temperature), the relative stabilities of the different solid phases may change, and solid-solid phase transformations may be thermodynamically favoured. In many cases, the transformation between two solid phases is reversible, although hysteresis is often observed (i.e., the observed phase transition temperature may differ depending on whether the phase transition occurs on cooling or heating).

Order-disorder phase transitions[3-5] are a class of solid-solid phase transformation in which a disordered structure undergoes a structural change on cooling across the phase transition temperature into a more ordered structure. In many cases, the disorder in the high-temperature phase is dynamic disorder, with the motion becoming "frozen" upon entering the ordered low-temperature phase (which is often associated with a reduction in crystal symmetry). In the case of organic solids, dynamic disorder in the high-temperature phase often takes the form of molecular reorientational processes, which cease to occur (or at least become significantly restricted) in the low-temperature phase. In some cases, the low-temperature phase may still exhibit some degree of static orientational disorder as a remnant of the dynamic disorder that existed in the high-temperature phase. Examples of organic materials that undergo such order-disorder phase transitions include rotator phase solids, in which highly symmetrical molecules [for example, hexamethylbenzene,[6-9] adamantane[10-16] and tetrakis(trimethylsilyl)silane[17-19]] undergo facile reorientational motions within their crystal structures in the high-temperature phase and transform to structures of lower symmetry in the low-temperature phase. Solid inclusion compounds (for example, urea[20-23] and thiourea[24-26] inclusion compounds) also exhibit order-disorder phase transitions in which dynamic disorder in the high-temperature phase concerns the reorientational motions of guest molecules inside a solid host structure, and the phase transition to the ordered phase is associated with "freezing" of the motion of the guest molecules and lowering of the symmetry of the host structure.

A common type of behaviour associated with order-disorder phase transitions[3-5,27] is for certain atomic sites in the crystal structure of the disordered high-temperature phase to be occupied by two (or more) different types of atom with essentially random occupancies as a consequence of a dynamic

process, recalling that crystal structures determined from diffraction data are a time-averaged representation of the true structure, and hence represent a time-average over any dynamic processes that occur in the material. In the low-temperature phase, the site occupancies become non-random, representing an increased degree of ordering (for example, as a consequence of "freezing" the dynamic process and the molecule adopting a specific preferred orientation in the crystal structure). This type of phase transition is exemplified by the material discussed in the present paper.

In this paper, we explore the temperature-dependent structural properties of 1,4-dibromo-2,3,5,6-tetramethylbenzene (DBTMB; Figure 1), demonstrating that this material undergoes a reversible order-disorder phase transition below ambient temperature. We report the temperature dependence of the structural properties, determined from single-crystal X-ray diffraction (XRD). The dynamic properties in the disordered high-temperature phase, established from natural-abundance solid-state ^{2}H NMR spectroscopy, are also reported.

It is relevant to note that polymorphism has been reported previously within the families of bromobenzenes and bromomethylbenzenes. For 1,2,4,5-tetrabromobenzene, a reversible thermosalient single-crystal to single-crystal phase transition has been reported[28-30] to occur at 46.5 °C. Polymorphism has also been reported for 1-bromo-2,3,5,6-tetramethylbenzene,[31] 1,4-dibromo-2,5-dimethylbenzene[32,33] and 1,3-dibromo-2,4,6-trimethylbenzene.[34]

2. Experimental

Synthesis of DBTMB was carried out following a literature procedure[35] with slight modifications. Chloroform (25 mL), 1,2,4,5-tetramethylbenzene (6.7 g, 0.05 mol) and aluminium chips (20 mg) were placed in a 250 mL flask and cooled to 0 ºC while stirring. Bromine (5.13 mL, 0.1 mol) was then added slowly to the flask and the solution was stirred for about 2 hr, yielding a crystalline precipitate. Chloroform (40 mL) was added to dissolve the product. The solution was filtered and cooled to 0 ºC to recover the colourless crystalline product (*ca*. 4.5 g). The product was identified as DBTMB [^{1}H NMR (400 MHz, $CDCl_3$): d 2.5 (s, 12H)].

Crystals of DBTMB suitable for single-crystal XRD were grown by slow evaporation of solvent (at ambient temperature over *ca*. 1 – 2 days) from a solution of DBTMB in methanol. The characteristic crystal morphology is needle-like, with an approximately rectangular cross section (in general, one side of the approximate rectangle is significantly longer than the other side).

Differential scanning calorimetry (DSC) data were recorded on a TA Instruments Q100 differential scanning calorimeter. The powder sample was ground lightly and loaded into a hermetically sealed aluminium pan. The DSC data were recorded with cooling/heating rates of 5 °C min^{-1} and 15 °C min^{-1}.

Single-crystal XRD data were recorded (Table 1) for a single crystal of DBTMB at ambient temperature (296 K) and at the following temperatures on cooling the crystal (the same crystal was studied at each temperature): 160 K, 150 K, 140 K, 130 K, 115 K, 100 K. Data were collected on an Agilent SuperNova Dual Atlas diffractometer (CuKα; λ = 1.5418 Å) equipped with a mirror monochromator and an Oxford Cryosystems cooling apparatus. Structure solution and refinement were carried out using SHELXS-86[36] and SHELXL[37] respectively. In the refinement, disorder of the bromine and methyl substituents of the DBTMB molecule was modelled by constraining the total occupancy of bromine and methyl groups on each substituent site to be equal to 1. In addition, the total occupancy of the bromine atoms in all six substituent sites was fixed at 2 and the total occupancy of the methyl groups in all six substituent sites was fixed at 4, consistent with the molecular formula $C_6Br_2(CH_3)_4$. For non-hydrogen atoms, anisotropic displacement parameters were refined. Hydrogen atoms were inserted according to standard geometries and a riding model was used for all hydrogen atoms with U_{iso} set at 1.2 or 1.5 times the value of U_{eq} for the carbon atom to which the hydrogen atom is bonded. Standard protocol was used for refinement of methyl groups. Methyl groups were initially free to rotate about the C–CH_3 bond but restraints on the orientation of the methyl groups relative to the aromatic ring were subsequently applied in cases for which convergence was not achieved.

Natural-abundance solid-state ^2H NMR data were recorded at ambient temperature (25 °C) on a Varian VNMRS solid-state NMR spectrometer (^2H Larmor frequency, 61.383 MHz). The data were recorded using magic-angle sample spinning (MAS) at two different MAS frequencies of 2 kHz (120,000 scans; total time, 33.3 hr) and 6 kHz (6,000 scans; total time, 1.7 hr), with high-power ^1H decoupling (TPPM) applied at 62.5 kHz (recycle delay, 1 s).

3. Results and Discussion

3.1 *Structural Properties*

Differential scanning calorimetry (DSC) data recorded for a powder sample of DBTMB (Figure 2) show that, on cooling from ambient temperature, an exothermic event occurs at *ca*. 152 – 154 K [–119.3 °C (153.8 K) at 5 °C min^{-1}; –121.5 °C (151.6 K) at 15 °C min^{-1}], and on subsequent heating, an endothermic event occurs at *ca*. 160 K [–113.6 °C (159.6 K) at both 5 °C min^{-1} and 15 °C min^{-1}]. These observations indicate the occurrence of a reversible phase transformation with slight hysteresis.

The crystal structure of DBTMB was determined from single-crystal XRD data recorded at several temperatures in the high-temperature and low-temperature phases (i.e., above and below *ca*. 154 K, respectively, on slow cooling) for the same single crystal. Structural data and refinement parameters at each temperature studied are given in Table 1, and cif files have been deposited at the Cambridge Crystallographic Data Centre (see Associated Content below).

In the high-temperature phase of DBTMB, the crystal structure (Figure 3) has monoclinic metric symmetry with space group $P2_1/c$ ($Z = 2$) and the following refined lattice parameters at 296 K: a = 8.3646(11) Å, b = 4.0140(4) Å, c = 17.382(3) Å, β = 117.518(15)°, V = 517.58(14) $Å^3$. The molecular arrangement in the crystal structure is similar to those found for other polyhalogenated benzenes.[38] The planar DBTMB molecules form stacks along the *b*-axis, which corresponds to the long axis of the needle-like crystal morphology. Along the stacks, strong π···π interactions exist between adjacent molecules with a distance of 4.01 Å (at 296 K) between the centres of adjacent molecules, corresponding to the periodic repeat distance along the *b*-axis. The normal to the aromatic ring is tilted by *ca*. 23° from the stacking axis to optimize the geometry of the π···π interactions. The perpendicular distance between aromatic planes is 3.70 Å.

In the high-temperature phase, the DBTMB molecule is located on a crystallographic inversion centre, and the asymmetric unit comprises half the molecule ($Z' = ½$). As a consequence, there are only three crystallographically distinct substituent sites. Each substituent site exhibits disorder in terms of occupancy by the bromine and methyl substituents. At 296 K, the refined occupancies of the bromine and methyl substituents at each site are: Br4/C4, 0.313(3)/0.687(3); Br5/C5, 0.359(3)/0.641(3); Br6/C6, 0.328(3)/0.672(3). Thus, for each of the three substituent sites, the occupancy of bromine is approximately 1/3 and the occupancy of the methyl group is approximately 2/3, consistent with statistical orientational disorder of the DBTMB molecule between six distinct orientations (we note that similar orientational disorder is observed in the crystal structures of other hexa-substituted benzenes, for example pentachloronitrobenzene[39,40]). For each molecular

orientation, the carbon atoms of the aromatic ring occupy an identical set of positions. The question of whether the orientational disorder in the high-temperature phase is static or dynamic is discussed below.

At the phase transition temperature (*ca*. 154 K on slow cooling), the crystal undergoes a single-crystal-to-single-crystal phase transition. The crystal structure of the low-temperature phase (Figure 4) remains monoclinic with space group $P2_1/c$, but the unit cell volume is increased by a factor of about 6 compared to the unit cell of the high-temperature phase. Compared to the unit cell of the high-temperature phase, the length of the *a*-axis of the low-temperature phase is increased by a factor of about 2, the length of the *b*-axis is increased by a factor of about 3, while the length of the *c*-axis and value of the β-angle are approximately unchanged.

At 150 K, the unit cell parameters are: a = 16.5482(8) Å, b = 11.8252(4) Å, c = 17.1772(9) Å, β = 117.259(7)°, V = 2988.0(3) Å^3. The number of DBTMB molecules in the unit cell is Z = 12, and the number of crystallographically independent molecules in the asymmetric unit is Z' = 3. As in the high-temperature phase, the DBTMB molecules form stacks along the *b*-axis, with π···π interactions between adjacent molecules in a given stack. For each molecule, the normal to the molecular plane is tilted by *ca*. 23° from the stacking axis to optimize π···π interactions. The distance between the centres of adjacent molecules along the stack (at 150 K) are 3.926 Å, 3.929 Å and 3.972 Å for the three independent distances along the stack. Interestingly, at all temperatures studied in the low-temperature phase, one intermolecular distance along the stack is significantly longer (by *ca*. 0.4 – 0.6 Å) than the other two distances. In contrast, in the high-temperature phase, all intermolecular (centre-to-centre) distances along the stack are equal (4.014 Å at 296 K), with neighbouring molecules related by translation along the stacking axis (*b*-axis).

For the three crystallographically independent molecules in the low-temperature phase, there are a total of 18 substituent sites. The transformation from the high-temperature phase to the low-temperature phase is accompanied by a substantial increase in ordering of the bromine and methyl substituents among the substituent sites, which become significantly more localized in the low-temperature phase leading to almost full occupancy (greater than *ca*. 0.90) of one type of substituent at each site (Figure 5). Subsequently, we refer to the substituent sites by the type of substituent with highest occupancy on the site. Within a given stack along the *b*-axis, the two sites with bromine substituents as the major component "rotate" in the manner of an approximate 3-fold helix on moving

along the *b*-axis; half of the stacks represent a right-handed helical arrangement and the other stacks represent a left-handed helical arrangement.

To assess the temperature dependence of the substituent site occupancies in the low-temperature phase, the crystal structure was determined at five different temperatures from 150 K to 100 K (on cooling the same single crystal). The occupancies of the major component for all 18 substituent sites (i.e., six substituent sites for each of the three independent molecules in the asymmetric unit) determined at each temperature are shown in Figure 5. At 150 K, the occupancy of the major component is greater than 0.90 for all substituent sites, ranging from 0.908(3) to 0.986(3). As temperature is decreased, there is a monotonic increase in the occupancy of the major component at each substituent site, and the range of occupancies becomes significantly narrower. Thus, at 100 K, the occupancy of the major component for all substituent sites is in the range from 0.969(3) to 0.997(1).

Molecules in adjacent stacks interact *via* van der Waals interactions involving the methyl and bromine substituents. In addition, favourable end-to-side Br···Br interactions exist between molecules in adjacent stacks. Within the *ac*-plane, groups of three molecules establish favourable end-to-side Br···Br interactions (Figure 6) giving rise to a triangular arrangement of three short Br···Br contacts with the following distances (at 150 K): Br3···Br1, 3.52 Å; Br1···Br5, 3.55 Å; Br5···Br3, 3.74 Å. This triangular motif involving three bromine substituents is well recognized in the context of halogen-bonding.[38,41-43] The other three bromine sites in the asymmetric unit are not engaged in Br···Br interactions of this type.

3.2 *Dynamic Properties*

Solid-state ^{2}H NMR is a powerful technique for studying reorientational motions of molecules in solids.[44-48] For ^{2}H nuclei in organic solids, the dominant anisotropic NMR interaction is the quadrupolar interaction, and a powder sample containing a random distribution of crystal orientations gives a characteristic broad-line ^{2}H NMR "powder pattern". Analysis of the ^{2}H NMR powder pattern allows the parameters that define the quadrupole interaction of the ^{2}H nucleus to be established, specifically the quadrupole coupling constant (χ) and asymmetry parameter (η). When reorientational motion involving the ^{2}H nucleus occurs at a rate greater than *ca.* 10^3 s^{-1}, the quadrupole interaction is influenced significantly by the reorientational motion, and the ^{2}H NMR powder pattern changes in

a well-defined manner. When the rate of motion is in the range 10^3 s^{-1} to 10^8 s^{-1}, analysis of the motionally averaged ^{2}H NMR powder pattern provides detailed information on both the mechanism of the molecular motion and the specific value of the rate of motion. When the rate of motion is higher than 10^8 s^{-1}, the geometry and mechanism of the motion can be deduced from analysis of the ^{2}H NMR powder pattern, but the specific rate of motion cannot be established (as discussed below, the dynamics of DBTMB in the high-temperature phase are within this so-called "rapid motion regime"). ^{2}H NMR lineshape analysis is generally carried out by calculating the lineshapes for proposed dynamic models, and finding the dynamic model for which the calculated ^{2}H NMR lineshape gives the best agreement with the experimental ^{2}H NMR lineshape.

In the present work, we have recorded the ^{2}H NMR spectrum for a sample of DBTMB with natural isotopic abundances. As described elsewhere,[49-57] given the very low natural abundance of the ^{2}H isotope (0.015%), it is advantageous to record the ^{2}H NMR spectrum for natural abundance samples under conditions of magic-angle sample spinning (MAS; the frequency of MAS is denoted ν_r). Under such circumstances, the broad-line ^{2}H NMR powder pattern is split into a set of narrow peaks separated by the spinning frequency ν_r, with the overall intensity envelope reflecting, at least approximately, the intensity distribution of the ^{2}H NMR powder pattern. To determine the dynamic model, the simulated ^{2}H NMR spectrum is calculated assuming a given dynamic model and at the same MAS frequency ν_r as the experimental ^{2}H NMR spectrum.

The natural-abundance solid-state ^{2}H NMR spectrum of DBTMB recorded at ambient temperature (25 °C) with MAS at ν_r = 2 kHz is shown in Figure 7a. The intensity distribution of the spinning sidebands is very similar to that observed previously in the same type of ^{2}H NMR measurement at the same MAS frequency for a sample of hexamethylbenzene with natural isotopic abundances.[49] From this observation, we deduce that the DBTMB molecules in the high-temperature phase may undergo similar dynamics to hexamethylbenzene, which has been studied extensively by solid-state NMR techniques.[9,49,50,58-60] In particular, the dynamic process involves rapid rotation of each methyl group about the C–CH_3 bond and rapid reorientation of the whole molecule by 60° jumps about an axis perpendicular to the plane of the aromatic ring (Figure 8). The simulated ^{2}H NMR spectrum for this dynamic model (for ν_r = 2 kHz) has been calculated assuming that both components of motion are in the rapid motion regime for ^{2}H NMR (i.e., rate of motion greater than *ca.* 10^8 s^{-1}), using motionally averaged values of the quadrupole interaction parameters consistent with those

reported in previous literature for hexamethylbenzene[9,50,58] (the best-fit simulated spectra shown in Figure 7 were obtained for the following values of the motionally averaged quadrupole interaction parameters: $\chi = 18.0$ kHz, $\eta = 0$). The excellent agreement between the simulated ^{2}H NMR spectrum (Figure 7b) and the experimental ^{2}H NMR spectrum (Figure 7a) recorded at 25 °C with $\nu_r = 2$ kHz confirms the validity of the proposed dynamic model at this temperature. The natural-abundance solid-state ^{2}H NMR spectrum was also recorded at 25 °C using a higher MAS frequency ($\nu_r = 6$ kHz; Figure 7c). Again, the simulated ^{2}H NMR spectrum (Figure 7d) calculated (for $\nu_r = 6$ kHz) on the assumption of the dynamic model discussed above is in excellent agreement with the experimental ^{2}H NMR spectrum (Figure 7c), giving further support to the veracity of the dynamic model.

4. Concluding Remarks

Although our ^{2}H NMR measurements were restricted only to ambient temperature, it is reasonable to suggest that the same dynamic model may be applicable throughout the high-temperature phase, although the rate of the 60° jump motion of the whole molecule is expected to decrease as temperature is decreased within this phase. We emphasize that the occurrence of the 60° jump motion of the whole molecule is fully consistent with the observation from our single-crystal XRD data that the occupancies of all substituent sites correspond to statistical occupancies (bromine occupancy *ca*. 1/3; methyl occupancy *ca*. 2/3) at both temperatures (296 K and 160 K) studied in the high-temperature phase.

For the low-temperature phase, the fact that the occupancies of the substituent sites differ significantly from the statistical occupancies suggests that there is now a significant energetic advantage for each of the three molecules in the asymmetric unit to adopt a specific orientation, although with a small residual population of each molecule in the other two (higher energy) orientations. Our observation that the population of the preferred orientation increases progressively as temperature is decreased within the low-temperature phase (see Figure 5) suggests that a dynamic process still exists in this phase, allowing a minor redistribution of site occupancies to occur as temperature is changed *via* reorientation of the molecule about an axis perpendicular to the plane of the aromatic ring. At this stage, we have not explored the dynamic properties of the low-temperature phase of DBTMB, but it is anticipated that the dynamic process allowing redistribution of the site

occupancies as a function of temperature is likely to be too slow to be probed by ^{2}H NMR lineshape analysis.

ASSOCIATED CONTENT

Accession Codes

CCDC 1583004 – 1583008 and CCDC 1583183 contain the supplementary crystallographic data for this paper. These data can be obtained free of charge via www.ccdc.cam.ac.uk/data_request/cif, or by emailing data_request@ccdc.cam.ac.uk, or by contacting The Cambridge Crystallographic Data Centre, 12 Union Road, Cambridge CB2 1EZ, UK; fax: +44 1223 336033.

AUTHOR INFORMATION

Corresponding Author

* E-mail: HarrisKDM@cardiff.ac.uk

ORCID

Kenneth D.M. Harris: 0000-0001-7855-8598

Notes

The authors declare no competing financial interest.

ACKNOWLEDGEMENTS

We are grateful to Cardiff University for general support and to Diamond Light Source for a Ph.D. studentship (to R. P.). R. S. thanks UGC (India) for a senior research fellowship and C. M. R. is grateful to Royal Society of Chemistry for a Researcher Mobility Grant (2015).

References

(1) Dunitz, J. D. Phase transitions in molecular crystals from a chemical viewpoint. *Pure Appl. Chem.* **1991**, *63*, 177-185.

(2) Bernstein, J. (2002). *Polymorphism in Molecular Crystals*. Oxford University Press.

(3) Parsonage, N. G.; Staveley, L. A. K. (1978). *Disorder in Crystals*. Oxford University Press.

(4) Sherwood, J. N. (Editor) (1979). *The Plastically Crystalline State: Orientationally Disordered Crystals*. John Wiley and Sons.

(5) Redfern, S. A. T. Order-disorder phase transitions. *Rev. Mineral. Geochem.* **2000**, *39*, 105-133.

(6) Andrew, E. R. Molecular motion in certain solid hydrocarbons. *J. Chem. Phys.* **1950**, *18*, 607-618.

(7) Hamilton, W. C.; Edmonds, J. W.; Tippe, A.; Rush, J. J. Methyl group rotation and the low temperature transition in hexamethylbenzene. Neutron diffraction study. *Discuss. Faraday Soc.* **1969**, *48*, 192-204.

(8) Celotti, G.; Bertinelli, F.; Stremmenos, C. Crystal symmetry and powder pattern of hexamethylbenzene below 116 K. *Acta Crystallogr. Sect. A* **1975**, *31*, 582-585.

(9) Tang, J.; Sterna, L.; Pines, A. Anisotropic spin-lattice relaxation of deuterated hexamethylbenzene. *J. Magn. Reson.* **1980**, *41*, 389-394.

(10) Nordman, C. E.; Schmitkons, D. L. Phase transition and crystal structures of adamantane. *Acta Crystallogr.* **1965**, *18*, 765-767.

(11) Resing, H. A. Confirmation of phase change in solid adamantane by N.M.R. *J. Chem. Phys.* **1965**, *43*, 1828-1829.

(12) Resing, H. A. NMR relaxation in adamantane and hexamethylenetetramine: diffusion and rotation. *Mol. Cryst. Liquid Cryst.* **1969**, *9*, 101-132.

(13) Graham, J. D.; Choi, J. K. NMR in the solid isomers twistane and adamantane. *J. Chem. Phys.* **1975**, *62*, 2509-2511.

(14) Meyer, M.; Ciccotti, G. Molecular dynamics simulation of plastic adamantane. I. Structural properties. *Mol. Phys.* **1985**, *56*, 1235-1248.

(15) Meyer, M.; Marhic, C.; Ciccotti, G. Molecular dynamics simulation of plastic adamantane. II. Reorientation motion. *Mol. Phys.* **1986**, *58*, 723-733.

(16) Amoureux, J. P.; Foulon, M. Comparison between structural analyses of plastic and brittle crystals. *Acta Crystallogr. Sect. B* **1987**, *43*, 470-479.

(17) Aliev, A. E.; Harris, K. D. M.; Apperley, D. C. High-resolution solid-state carbon-13 and silicon-29 NMR investigations of the dynamic properties of tetrakis(trimethylsilyl)silane. *J. Chem. Soc. Chem. Commun.* **1993**, 251-253.

(18) Jones, M. J.; Guillaume, F.; Harris, K. D. M.; Dianoux, A.-J. Molecular dynamics of tetrakis(trimethylsilyl)silane in the solid state: an incoherent quasi-elastic neutron scattering investigation. *Proc. Royal Soc. A* **1996**, *452*, 701-714.

(19) Dinnebier, R. E.; Dollase, W. A.; Helluy, X.; Kummerlen, J.; Sebald, A.; Schmidt, M. U.; Pagola, S.; Stephens, P. W.; van Smaalen, S. Order-disorder phenomena determined by high-resolution powder diffraction: the structures of tetrakis(trimethylsilyl)methane $C[Si(CH_3)_3]_4$

and tetrakis(trimethylsilyl)silane $Si[Si(CH_3)_3]_4$. *Acta Crystallogr. Sect. B* **1999**, *55*, 1014-1029.

(20) Harris, K. D. M.; Jonsen, P. Deuteron NMR investigation of the dynamic behavior of *n*-hexadecane in its urea inclusion compound. *Chem. Phys. Lett.* **1989**, *154*, 593-598.

(21) Guillaume, F.; Smart, S. P.; Harris, K. D. M.; Dianoux, A. J. Neutron scattering investigations of guest molecular dynamics in α,ω-dibromoalkane-urea inclusion compounds. *J. Phys.: Condens. Matter* **1994**, *6*, 2169-2184.

(22) Aliev, A. E.; Smart, S. P.; Shannon, I. J.; Harris, K. D. M. Structural and dynamic properties of the 1,10-dibromodecane/urea inclusion compound, investigated by variable-temperature powder X-ray diffraction, solid-state ^2H NMR lineshape analysis and solid-state ^2H NMR spin-lattice relaxation time measurements. *J. Chem. Soc. Faraday Trans.* **1996**, *92*, 2179-2185.

(23) Yeo, L.; Kariuki, B. M.; Serrano-Gonzalez, H.; Harris, K. D. M. Structural properties of the low-temperature phase of the hexadecane/urea inclusion compound, investigated by synchrotron X-ray powder diffraction. *J. Phys. Chem. B* **1997**, *101*, 9926-9931.

(24) Desmedt, A.; Kitchin, S. J.; Guillaume, F.; Couzi, M.; Harris, K. D. M.; Bocanegra, E. H. Phase transitions and molecular dynamics in the cyclohexane/thiourea inclusion compound. *Phys. Rev. B* **2001**, *64*, 054106.

(25) Pan, Z.; Desmedt, A.; MacLean, E. J.; Guillaume, F.; Harris, K. D. M. Structural properties of low-temperature phase transitions in the prototypical thiourea inclusion compound: cyclohexane/thiourea. *J. Phys. Chem. C* **2008**, *112*, 839-847.

(26) Palmer, B. A.; Kariuki, B. M.; Morte-Rodenas, A.; Harris, K. D. M. Structural rationalization of the phase transition behavior in a solid organic inclusion compound: bromocyclohexane/thiourea. *Cryst. Growth Des.* **2012**, *12*, 577-582.

(27) Chia, T. S.; Quah, C. K. Temperature-induced order-disorder structural phase transitions of two-dimensional isostructural hexamethylenetetramine co-crystals. *Acta Crystallogr. Sect. B* **2017**, *73*, 879-890.

(28) Gafner, G.; Herbstein, F. H. The crystal and molecular structures of overcrowded halogenated compounds. II. β-1,2,4,5-Tetrabromobenzene. *Acta Crystallogr.* **1960**, *13*, 706-716.

(29) Gafner, G.; Herbstein, F. H. The crystal and molecular structures of overcrowded halogenated compounds. V. γ-l,2,4,5-Tetrabromobenzene. *Acta Crystallogr.* **1964**, *17*, 982-985.

(30) Sahoo, S. C.; Sinha, S. B.; Kiran, M. S. R. N.; Ramamurty, U.; Dericioglu, A. F.; Reddy, C. M.; Naumov, P. Kinematic and mechanical profile of the self-actuation of thermosalient crystal twins of 1,2,4,5-tetrabromobenzene: A molecular crystalline analogue of a bimetallic strip. *J. Am. Chem. Soc.* **2013**, *135*, 13843-13850.

(31) Charbonneau, G.; Baudour, J.; Messager, J. C.; Meinnel, J. Polymorphism of 1-bromo-2,3,4,6-tetramethylbenzene. *Bull. Soc. Fr. Mineral. Cristallogr.* **1965**, *88*, 147-148.

(32) Reiter, S. A.; Nogai, S. D.; Schmidbaur, H. Preparation, structure and gold(I) complexation of p-xylylene-1,4-diphosphines. *Z. Naturforsch. B: Chem. Sci.* **2005**, *60*, 511-519.

(33) Jones, P. G.; Kus, P. A new polymorph of 1,4-dibromo-2,5-dimethylbenzene: H...Br and Br...π versus Br...Br interactions. *Acta Crystallogr. Sect. C* **2011**, *67*, o131-o133.

(34) Hernandez, O.; Cousson, A.; Plazanet, M.; Nierlich, M.; Meinnel, J. The low-temperature phase of 1,3-dibromo-2,4,6-trimethylbenzene: a single-crystal neutron diffraction study at 120 and 14 K. *Acta Crystallogr. Sect. C* **2003**, *59*, o445-o450.

(35) Usta, H.; Kim, C.; Wang, Z.; Lu, S.; Huang, H.; Facchetti, A.; Marks, T. J. Anthracenedicarboximide-based semiconductors for air-stable, n-channel organic thin-film transistors: materials design, synthesis, and structural characterization. *J. Mater. Chem.* **2012**, *22*, 4459-4472.

(36) Sheldrick, G. M. Phase annealing in SHELX-90: direct methods for larger structures. *Acta Crystallogr. Sect. A* **1990**, *46*, 467-473.

(37) Sheldrick, G. M. Crystal structure refinement with SHELXL. *Acta Crystallogr. Sect. C* **2015**, *71*, 3-8.

(38) Reddy, C. M.; Kirchner, M. T.; Gundakaram, R. C.; Padmanabhan, K. A.; Desiraju, G. R. Isostructurality, polymorphism and mechanical properties of some hexahalogenated benzenes: the nature of halogen···halogen interactions. *Chem. Eur. J.* **2006**, *12*, 2222-2234.

(39) Tanaka, I.; Iwasaki, F.; Aihara, A. Crystal structure of pentachloronitrobenzene. *Acta Crystallogr. Sect. B* **1974**, *30*, 1546-1549.

(40) Thomas, L. H.; Welberry, T. R.; Goossens, D. J.; Heerdegen, A. P.; Gutmann, M. J.; Teat, S. J.; Lee, P. L.; Wilson, C. C.; Cole, J. M. Disorder in pentachloronitrobenzene, $C_6Cl_5NO_2$: a diffuse scattering study. *Acta Crystallogr. Sect. B* **2007**, *63*, 663-673.

(41) Anthony, A.; Desiraju, G. R.; Jetti, R. K. R.; Kuduva, S. S.; Madhavi, N. N. L.; Nangia, A.; Thaimattam, R.; Thalladi, V. R. Crystal engineering: some further strategies. *Cryst. Eng.* **1998**, *1*, 1-18.

(42) Lu, Y.; Zou, J.; Wang, H.; Yu, Q.; Zhang, H.; Jiang, Y. Triangular halogen trimers. A DFT study of the structure, cooperativity, and vibrational properties. *J. Phys. Chem. A* **2005**, *109*, 11956-11961.

(43) Cavallo, G.; Metrangolo, P.; Milani, R.; Pilati, T.; Priimagi, A.; Resnati, G.; Terraneo, G. The halogen bond. *Chem. Rev.* **2016**, *116*, 2478-2601.

(44) Seelig, J. Deuterium magnetic resonance: theory and application to lipid membranes. *Quart. Rev. Biophys.* **1977**, *10*, 353-418.

(45) Jelinski, L. W. Solid state deuterium NMR studies of polymer chain dynamics. *Ann. Rev. Mater. Sci.* **1985**, *15*, 359-377.

(46) Vold, R. R.; Vold, R. L. Deuterium relaxation in molecular solids. *Adv. Magn. Opt. Reson.* **1991**, *16*, 85-171.

(47) Hoatson, G. L.; Vold, R. L. *NMR Basic Principles and Progress* **1994,** *32*, 3.

(48) Aliev, A. E.; Harris, K. D. M. Probing hydrogen bonding in solids using solid state NMR spectroscopy. *Struct. Bonding* **2004**, *108*, 1-53.

(49) Aliev, A. E.; Harris, K. D. M.; Apperley, D. C. Natural abundance high-resolution solid state ^{2}H NMR spectroscopy. *Chem. Phys. Lett.* **1994**, *226*, 193-198.

(50) Poupko, R.; Olender, Z.; Reichert, D.; Luz, Z. Deuterium MAS NMR in natural abundance. *J. Magn. Reson. Ser. A* **1994**, *106*, 113-115.

(51) Aliev, A. E.; Harris, K. D. M. Natural abundance solid state ^{2}H NMR studies of phase transitions in rotator phase solids. *Mendeleev Commun.* **1993**, 153-155.

(52) Reichert, D.; Olender, Z.; Poupko, R.; Zimmermann, H.; Luz, Z. Deuterium two-dimensional exchange nuclear magnetic resonance by rotor-synchronized magic-angle spinning. *J. Chem. Phys.* **1993**, *98*, 7699-7710.

(53) Gerardy-Montouillout, V.; Malveau, C.; Tekely, P.; Olender, Z.; Luz, Z. ODESSA, a new 1D NMR exchange experiment for chemically equivalent nuclei in rotating solids. *J. Magn. Reson. Ser. A* **1996**, *123*, 7-15.

(54) Malveau, C.; Tekely, P.; Canet, D. Visualization of residual anisotropic interactions in crosslinked natural rubbers by dipolar local field measurements and ^{2}H natural abundance NMR spectroscopy. *Solid State Nucl. Magn. Reson.* **1997**, *7*, 271-280.

(55) Mizuno, T.; Nemoto, T.; Tansho, M.; Shimizu, T.; Ishii, H.; Takegoshi, K. ^{2}H Natural-abundance MAS NMR spectroscopy: an alternative approach to obtain ^{1}H chemical shifts in solids. *J. Am. Chem. Soc.* **2006**, *128*, 9683-9686.

(56) Lesot, P.; Courtieu, J. Natural abundance deuterium NMR spectroscopy. Developments and analytical applications in liquids, liquid crystals and solid phases. *Prog. Nucl. Magn. Reson. Spectrosc.* **2009**, *55*, 128-159.

(57) Aliev, A. E.; Mann, S. E.; Iuga, D.; Hughes, C. E.; Harris, K. D. M. Natural-abundance solid-state ^{2}H NMR spectroscopy at high magnetic field. *J. Phys. Chem. A* **2011**, *115*, 5568-5578.

(58) Schwartz, L. J.; Meirovitch, E.; Ripmeester, J. A.; Freed, J. H. Quadrupole echo study of internal motions in polycrystalline media. *J. Phys. Chem.* **1983**, *87*, 4453-4461.

(59) Jansen-Glaw, B.; Roessler, E.; Taupitz, M.; Vieth, H. M. Hexamethylbenzene as a sensitive nuclear magnetic resonance probe for studying organic crystals and glasses. *J. Chem. Phys.* **1989**, *90*, 6858-6866.

(60) Hoatson, G. L.; Vold, R. L.; Tse, T. Y. Individual spectral densities and molecular motion in polycrystalline hexamethylbenzene-d_{18}. *J. Chem. Phys.* **1994**, *100*, 4756-4765.

Table 1 Crystal structure and refinement data for DBTMB at several temperatures in the high-temperature (HT) and low-temperature (LT) phases.

	$C_{10}H_{12}Br_2$						
FW	292.02						
System	Monoclinic						
Space group	$P2_1/c$						
λ / Å	1.54184						
Size / mm^3	0.599 × 0.074 × 0.061						
T / K	100(2)	115(2)	130(2)	140(2)	150(2)	160(2)	296(2)
Phase	LT	LT	LT	LT	LT	HT	HT
a / Å	16.5037(5)	16.5234(5)	16.5416(5)	16.5498(6)	16.5482(8)	8.2901(12)	8.3646(11)
b / Å	11.7773(3)	11.7905(3)	11.8140(3)	11.8204(3)	11.8252(4)	3.9439(5)	4.0140(4)
c / Å	17.1364(5)	17.1484(5)	17.1647(5)	17.1725(6)	17.1772(9)	17.197(2)	17.382(3)
α / °	90	90	90	90	90	90	90
β / °	117.204(4)	117.234(4)	117.255(4)	117.258(4)	117.259(7)	117.258(13)	117.518(15)
γ / °	90	90	90	90	90	90	90
V / $Å^3$	2962.35(17)	2970.49(17)	2981.96(17)	2986.33(19)	2988.0(3)	499.82(13)	517.58(14)
Z	12	12	12	12	12	2	2
ρ_{cal} / Mg m^{-3}	1.964	1.959	1.951	1.948	1.947	1.940	1.874
Number of Reflections	11150	10247	10248	11100	11483	1509	1578
Unique Data	5859	5848	5855	5891	5881	959	997
R(int)	0.0323	0.0274	0.0288	0.0294	0.0441	0.0657	0.0710
Gof	1.064	1.048	1.038	1.036	1.018	1.049	1.046
R1 [I>2σ(I)]	0.0402	0.0433	0.0438	0.0437	0.0479	0.0630	0.0607
wR2 [I>2σ(I)]	0.1088	0.1157	0.1185	0.1174	0.1262	0.1729	0.1818
R1 (all data)	0.0456	0.0499	0.0511	0.0515	0.0573	0.0671	0.0689
wR2(all data)	0.1156	0.1243	0.1276	0.1264	0.1396	0.1782	0.1959

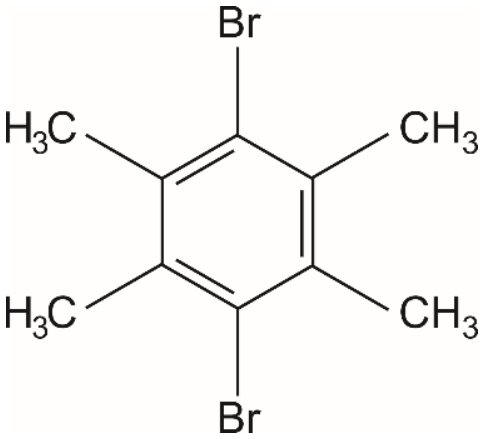

Figure 1 Molecular structure of DBTMB.

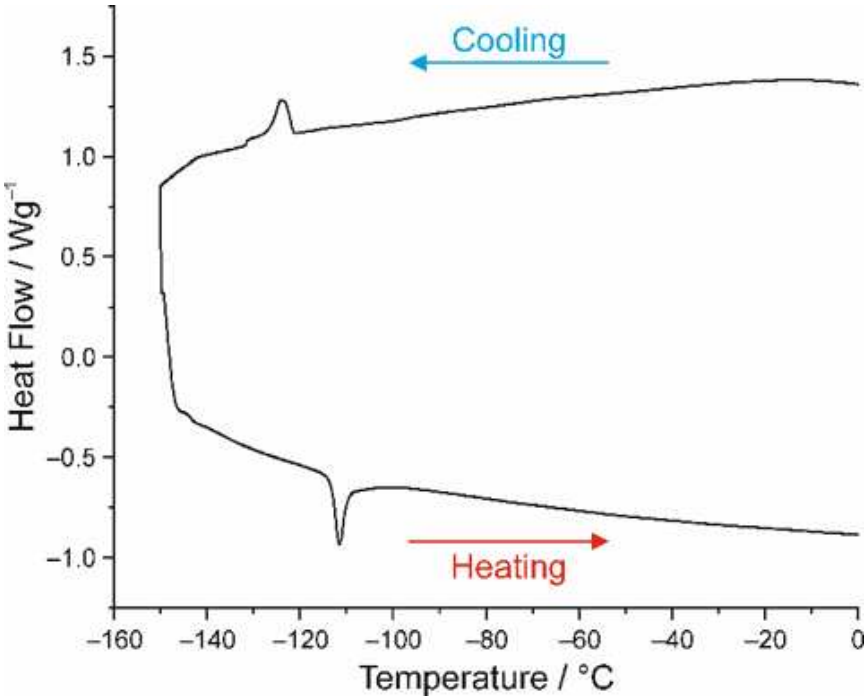

Figure 2 DSC data recorded for DBTMB (cooling/heating rate, 15 °C min^{-1}). Heat flow is positive for exothermic processes and negative for endothermic processes.

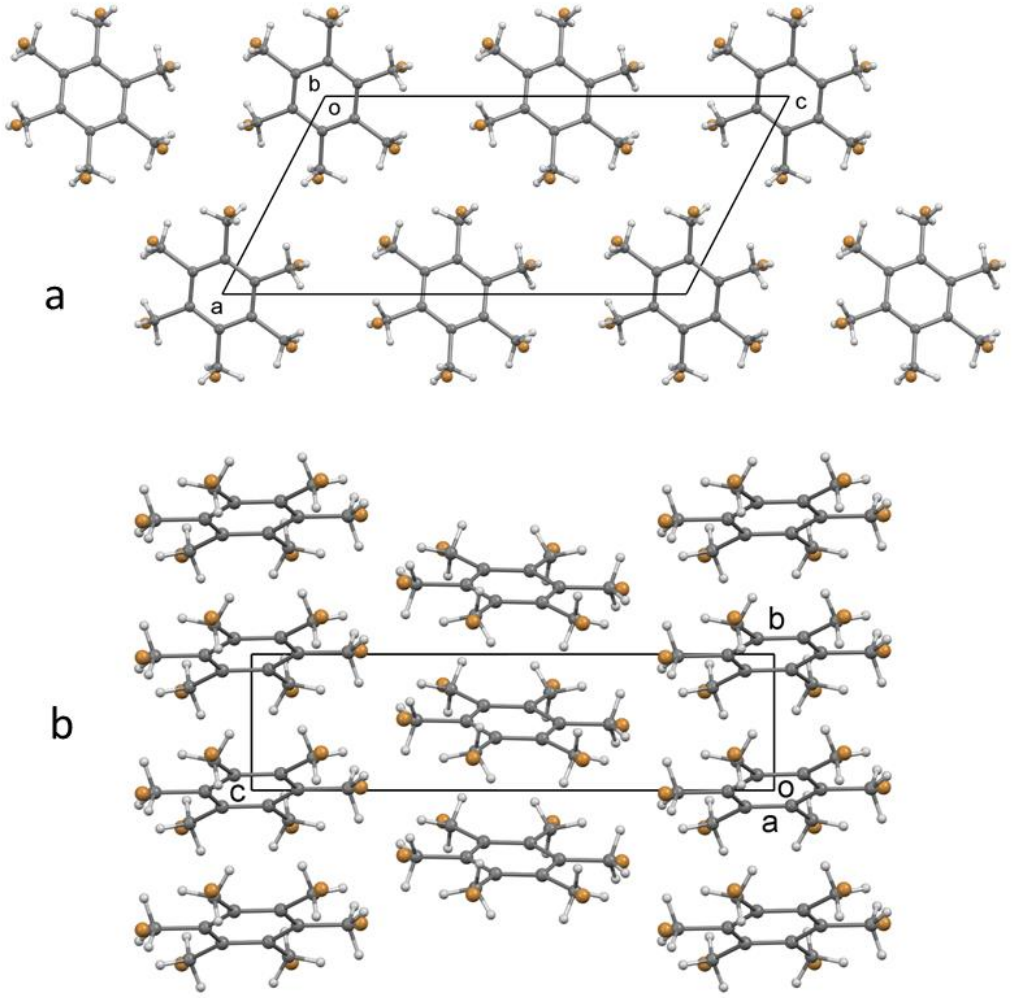

Figure 3 Crystal structure of DBTMB at 296 K viewed: (a) along the *b*-axis (parallel to the stacking axis), and (b) along the *a*-axis (perpendicular to the stacking axis, which runs vertically). Each substituent position on the aromatic ring is disordered and occupied by both bromine (occupancy *ca*. 1/3) and methyl (occupancy *ca*. 2/3) substituents.

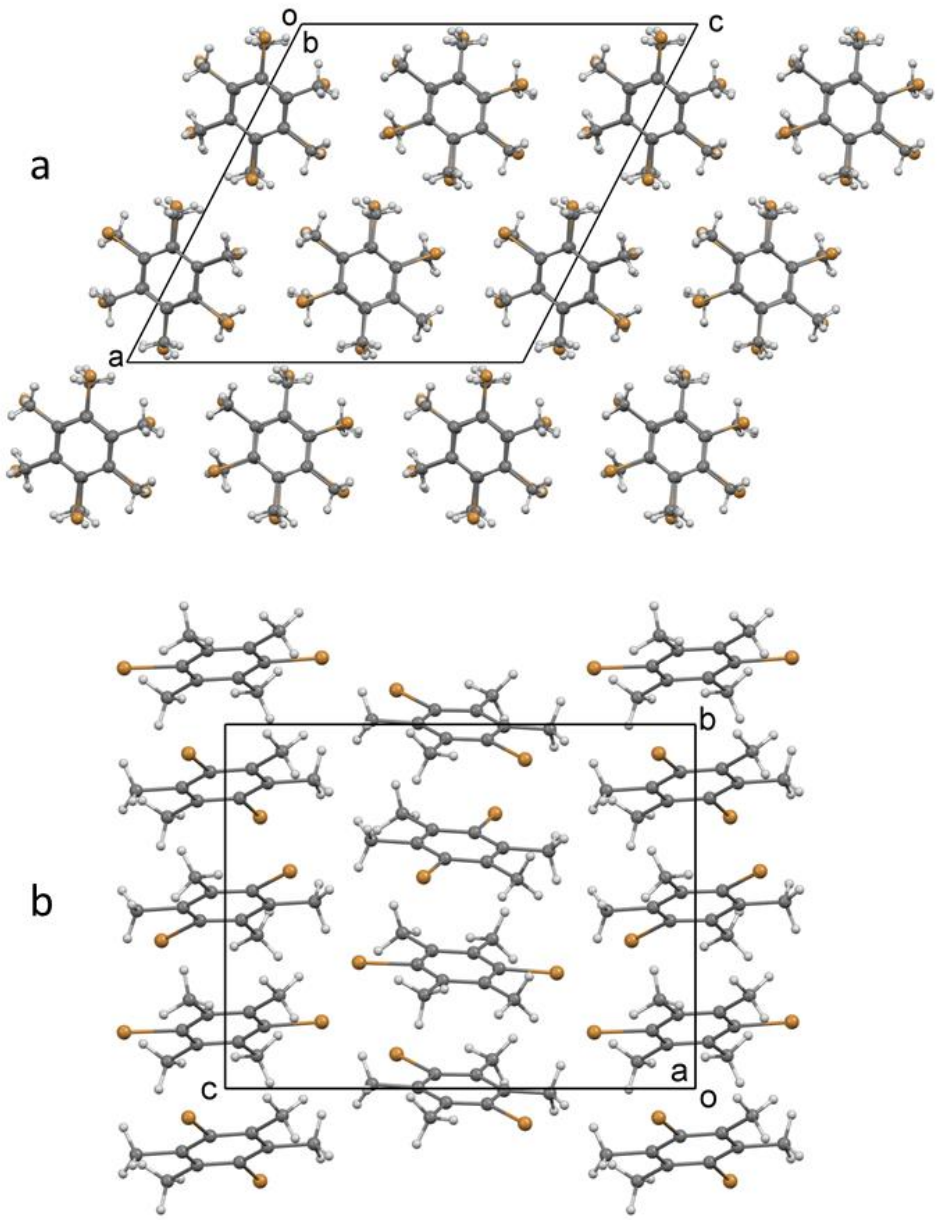

Figure 4 Crystal structure of the low-temperature phase of DBTMB at 150 K, viewed: (a) along the *b*-axis (parallel to the stacking axis), and (b) along the *a*-axis (perpendicular to the stacking axis, which runs vertically). For each substituent site, only the substituent of highest occupancy (greater than *ca*. 0.90) is shown. In (a), the full crystal structure is shown, while in (b), only a single layer of stacks parallel to the *bc*-plane is shown. It is clear from (b) that the three independent molecules along the stack have different molecular orientations.

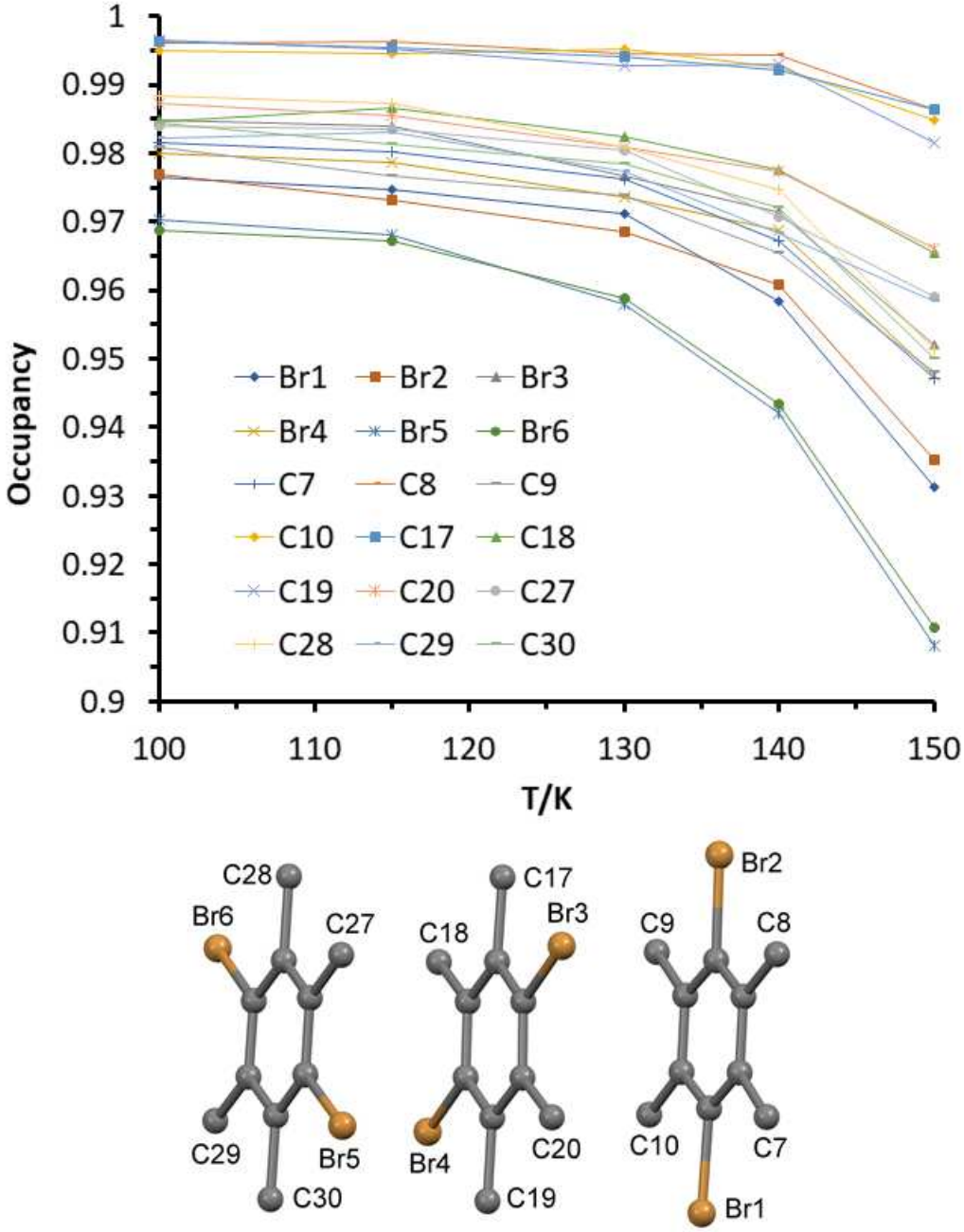

Figure 5 Occupancy of the major component in each of the 18 substituent positions in the crystal structure of the low-temperature phase of DBTMB determined as a function of temperature on cooling from 150 K to 100 K.

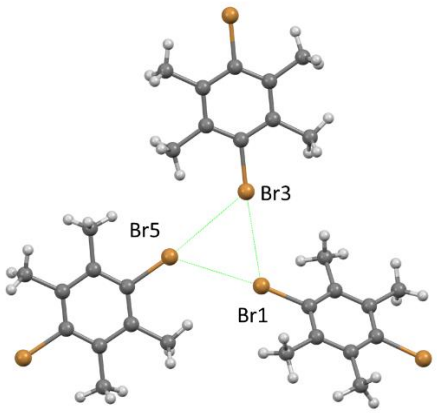

Figure 6 A group of three molecules linked by intermolecular Br···Br contacts in the crystal structure of the low-temperature phase of DBTMB at 150 K. Only the molecular orientations of higher occupancy are shown.

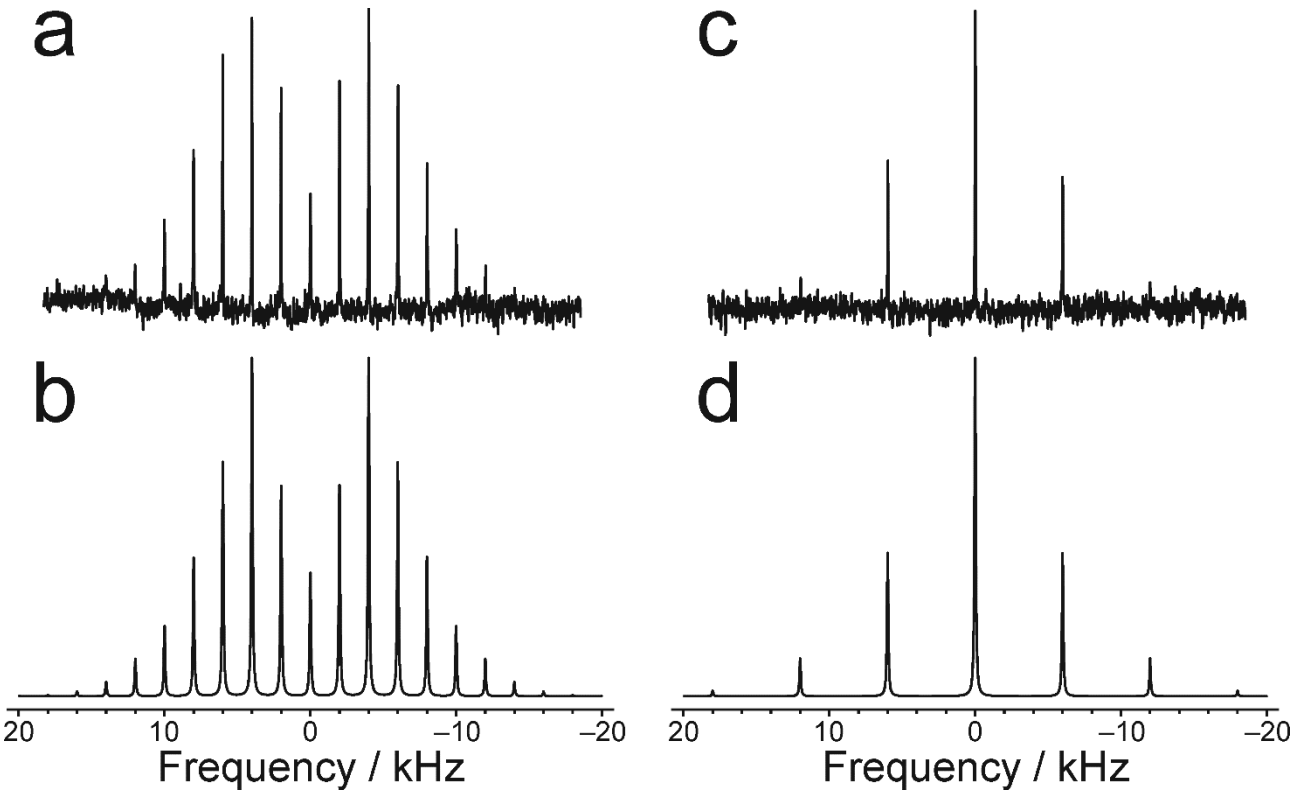

Figure 7 Experimental solid-state ^{2}H NMR spectra recorded at 25 °C for a powder sample of DBTMB with natural isotopic abundances at MAS frequencies of (a) 2 kHz and (c) 6 kHz. Simulated solid-state ^{2}H NMR spectra calculated for the dynamic model of the DBTMB molecule shown in Figure 7 at MAS frequencies of (b) 2 kHz and (d) 6 kHz.

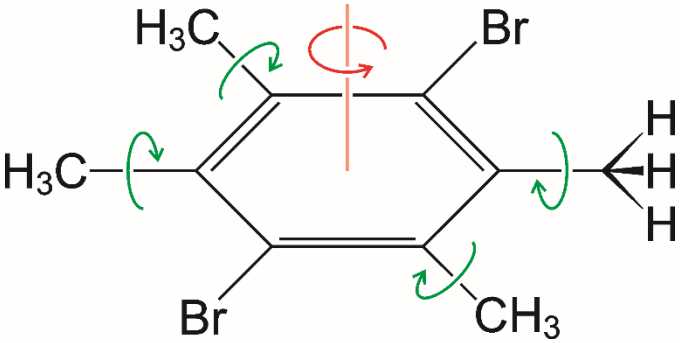

Figure 8 Dynamic model for DBTMB in the high-temperature phase, involving rapid rotation of each methyl group about the C–CH_3 bond (green arrows) and rapid reorientation of the whole molecule by 60° jumps about an axis perpendicular to the plane of the aromatic ring (red arrow).

For Table of Contents Use Only

Temperature-Dependent Structural Properties, Phase Transition Behaviour and Dynamic Properties of a Benzene Derivative in the Solid State

Yating Zhou, Rhian Patterson, P. Andrew Williams, Benson M. Kariuki, Colan E. Hughes, Ranita Samanta, Ramesh Devarapalli, C. Malla Reddy, David C. Apperley, Kenneth D. M. Harris*

TOC Graphic

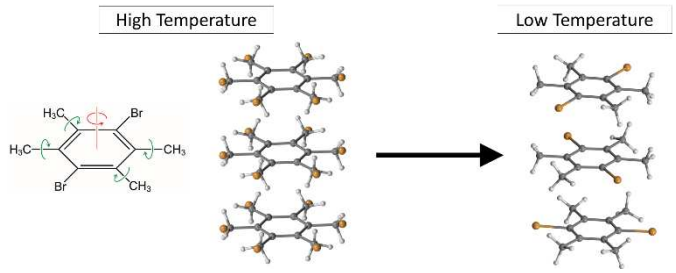

Synopsis

Solid-state structural studies show that 1,4-dibromo-2,3,5,6-tetramethylbenzene undergoes an order-disorder phase transition at *ca*. 154 K. In the high-temperature phase, bromine and methyl groups are distributed among the six substituent sites with statistical occupancies; solid-state ^{2}H NMR shows that this disorder is dynamic. In the low-temperature phase, bromine and methyl groups occupy preferred sites, becoming progressively more ordered as temperature decreases.